


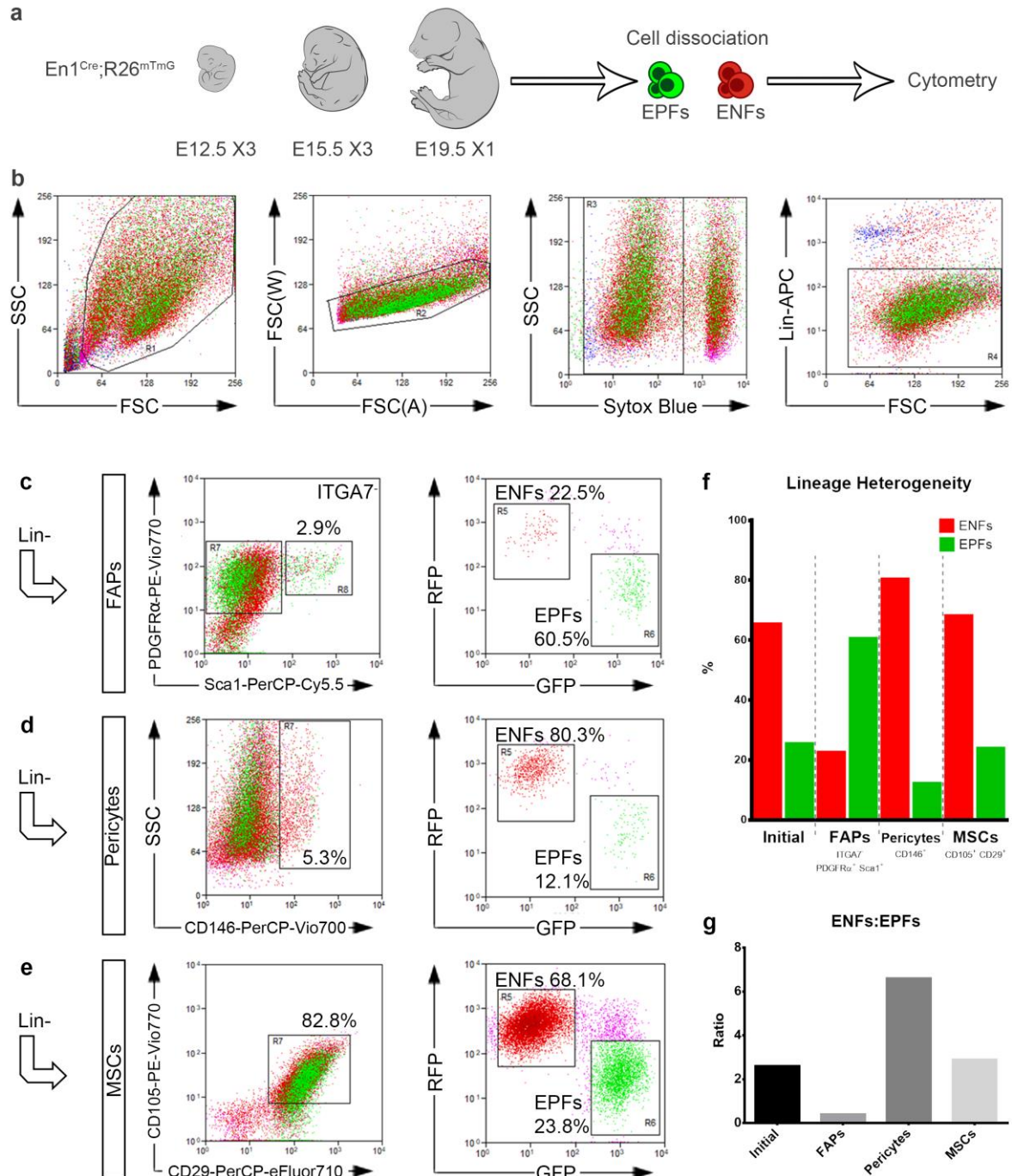
In the format provided by the authors and unedited.

# Two succeeding fibroblastic lineages drive dermal development and the transition from regeneration to scarring

Dongsheng Jiang<sup>1,5</sup>, Donovan Correa-Gallegos<sup>1,5</sup>, Simon Christ<sup>1,5</sup>, Ania Stefanska<sup>1</sup>, Juan Liu<sup>1</sup>, Pushkar Ramesh<sup>1</sup>, Vijayanand Rajendran<sup>1</sup>, Martina M. De Santis<sup>1,2,3</sup>, Darcy E. Wagner<sup>1,2,3,4</sup>  and Yuval Rinkevich<sup>1,4</sup> \*

<sup>1</sup>Comprehensive Pneumology Centre/Institute of Lung Biology and Disease, Helmholtz Zentrum München, Munich, Germany. <sup>2</sup>Department of Experimental Medical Sciences, Lund University, Lund, Sweden. <sup>3</sup>Wallenberg Centre for Molecular Medicine, Lund University, Lund, Sweden.

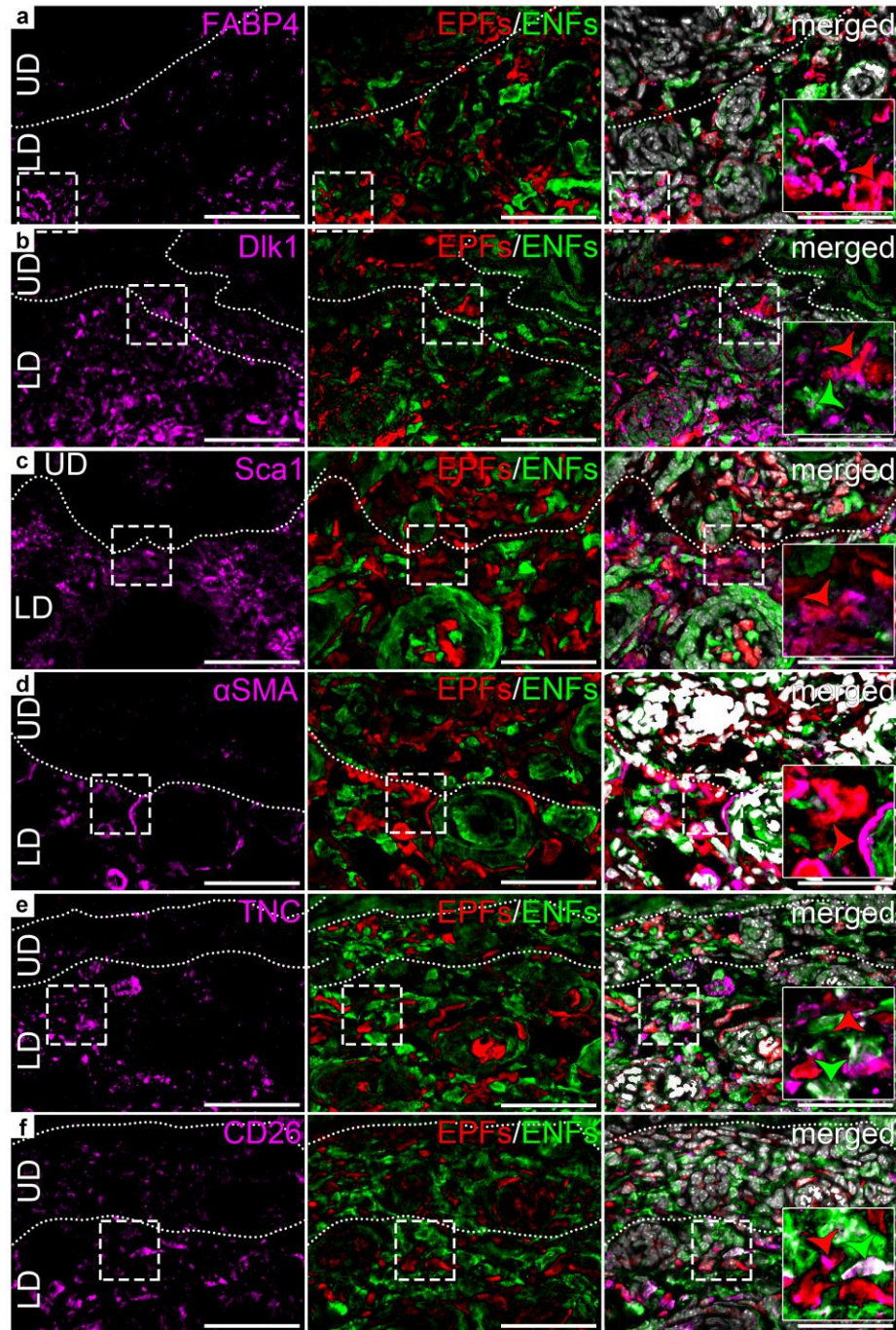
<sup>4</sup>Member of the German Centre for Lung Research (DZL), Munich, Germany. <sup>5</sup>These authors contributed equally: Dongsheng Jiang, Donovan Correa-Gallegos and Simon Christ. \*e-mail: [yuval.rinkevich@helmholtz-muenchen.de](mailto:yuval.rinkevich@helmholtz-muenchen.de)



### Supplementary Figure 1

Flow cytometric analysis of mesenchymal markers on ENFs and EPFs.

**a**, single cell suspension was prepared from the pooled back-skin from three E12.5, three E15.5 and one E19.5 *En1<sup>Cre</sup>;R26<sup>mTmG</sup>* embryos, and subjected to flow cytometric analysis. **b**, Sytox blue was used to exclude dead cells, and APC-conjugated lineage markers (CD45, CD31, Ter119, EpCAM, Tie-2, Lyve-1) were used to exclude non-mesenchymal cells. **c-e**, representative analysis plots of fibro-adipogenic progenitors (FAPs) (Lin<sup>-</sup>ITGA7<sup>+</sup>Sca1<sup>+</sup>PDGFRα<sup>+</sup>) (c), pericytes (Lin<sup>-</sup>CD146<sup>+</sup>) (d), and mesenchymal stem cells (Lin<sup>-</sup>CD29<sup>+</sup>CD105<sup>+</sup>) (e), and their distributions in ENFs and EPFs. **f-g**, the percentages of ENFs and EPFs (f) and the ratio of ENFs:EPFs (g) within Lin<sup>-</sup> cells (initial), FAPs, pericytes and MSCs.

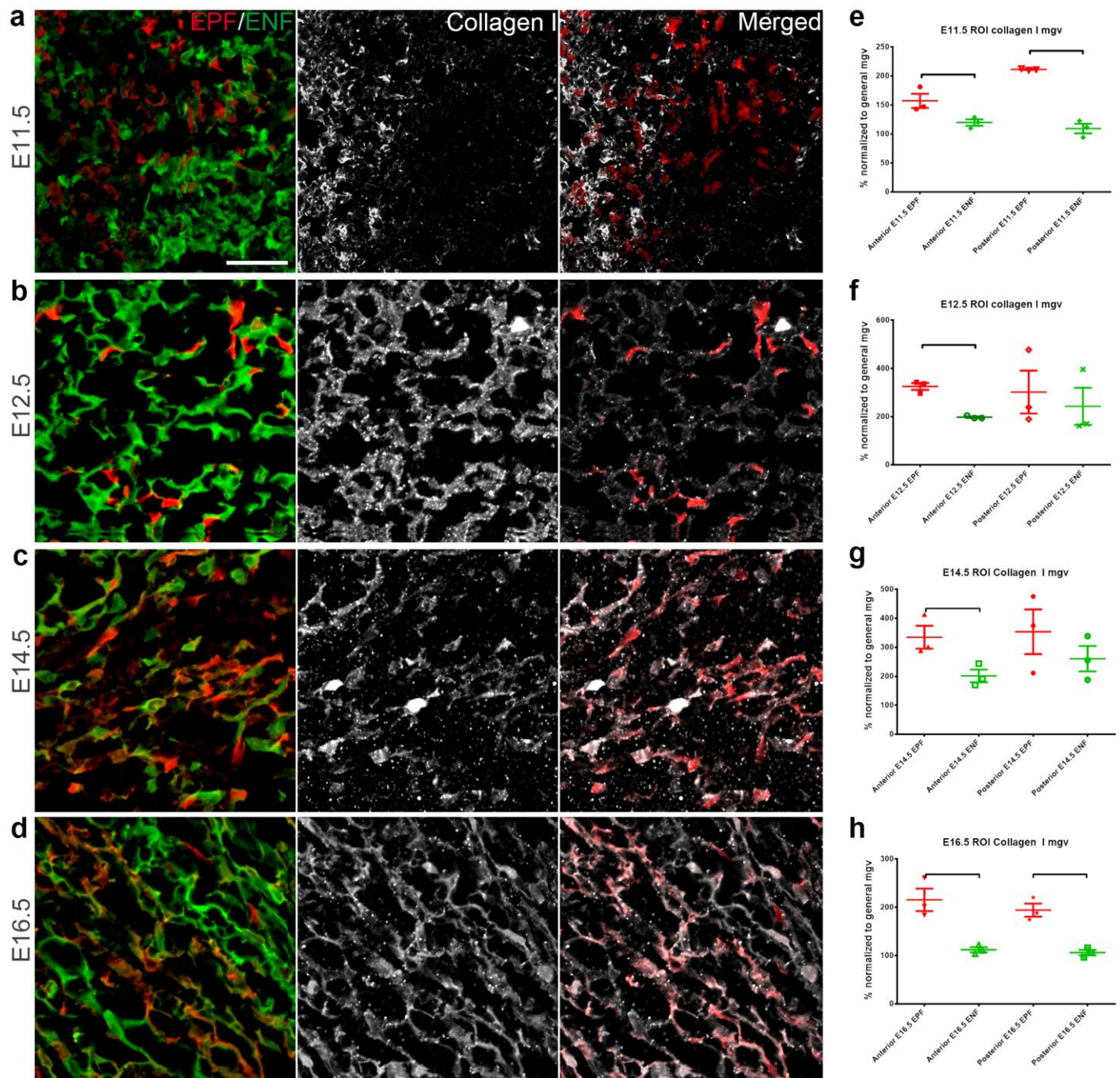


### Supplementary Figure 2

Expression of mesoderm markers on ENFs and EPFs by immunofluorescence staining.

Cryosections were prepared from *En1<sup>Cre</sup>;R26<sup>VT2/GK3</sup>* neonates (P1), and stained with primary antibodies against mouse FABP4 (a), Dlk1 (b), Sca1 (c),  $\alpha$ SMA (d), TNC (e), and CD26 (f), and AF647-conjugated respective secondary antibodies. Depicted are representative high-power images of AF647 channel for antibodies (left), GFP-RFP channels for ENFs-EPFs (middle), and merged channels (right). Dotted lines indicate the border of epidermis and dermis, and the border of upper dermis (UD) and lower dermis (LD). Squares indicate the locations of enlarged inserts in merged images. Scales: 50  $\mu$ m. The depicted are representative images of three individual embryos.

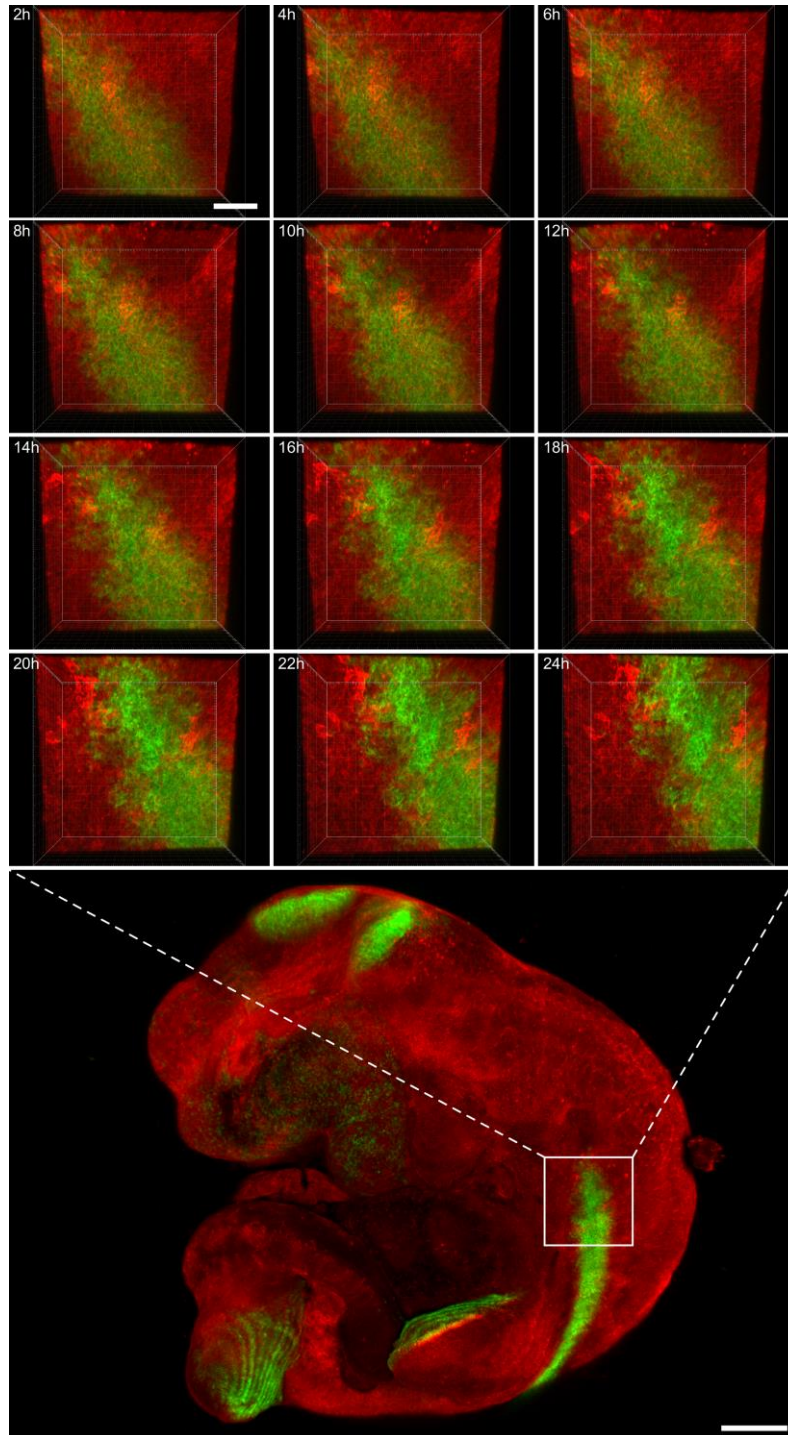




### Supplementary Figure 3

EPFs associate with Collagen I fibers.

a-d, Immunofluorescence for Collagen I of E11.5 (a), E12.5 (b), E14.5 (c), or E16.5 (d) *En1<sup>Cre</sup>;R26<sup>VT2/GK3</sup>* embryos. e-h, EPF- or ENF-signal-derived ROI mean grey value (mgv)  $\pm$  SEM of the Collagen I signal from anterior or posterior regions of E11.5 (e), E12.5 (f), E14.5 (g), or E16.5 (h) *En1<sup>Cre</sup>;R26<sup>VT2/GK3</sup>* embryos. n = 3 optical fields of anterior and posterior regions at each development stage. Two-tailed unpaired *t*-test. \*  $p < 0.05$ . Scale: 50  $\mu$ m. Images represent 1 out of three optical fields. The exact p values are listed in Supplementary Table 1.

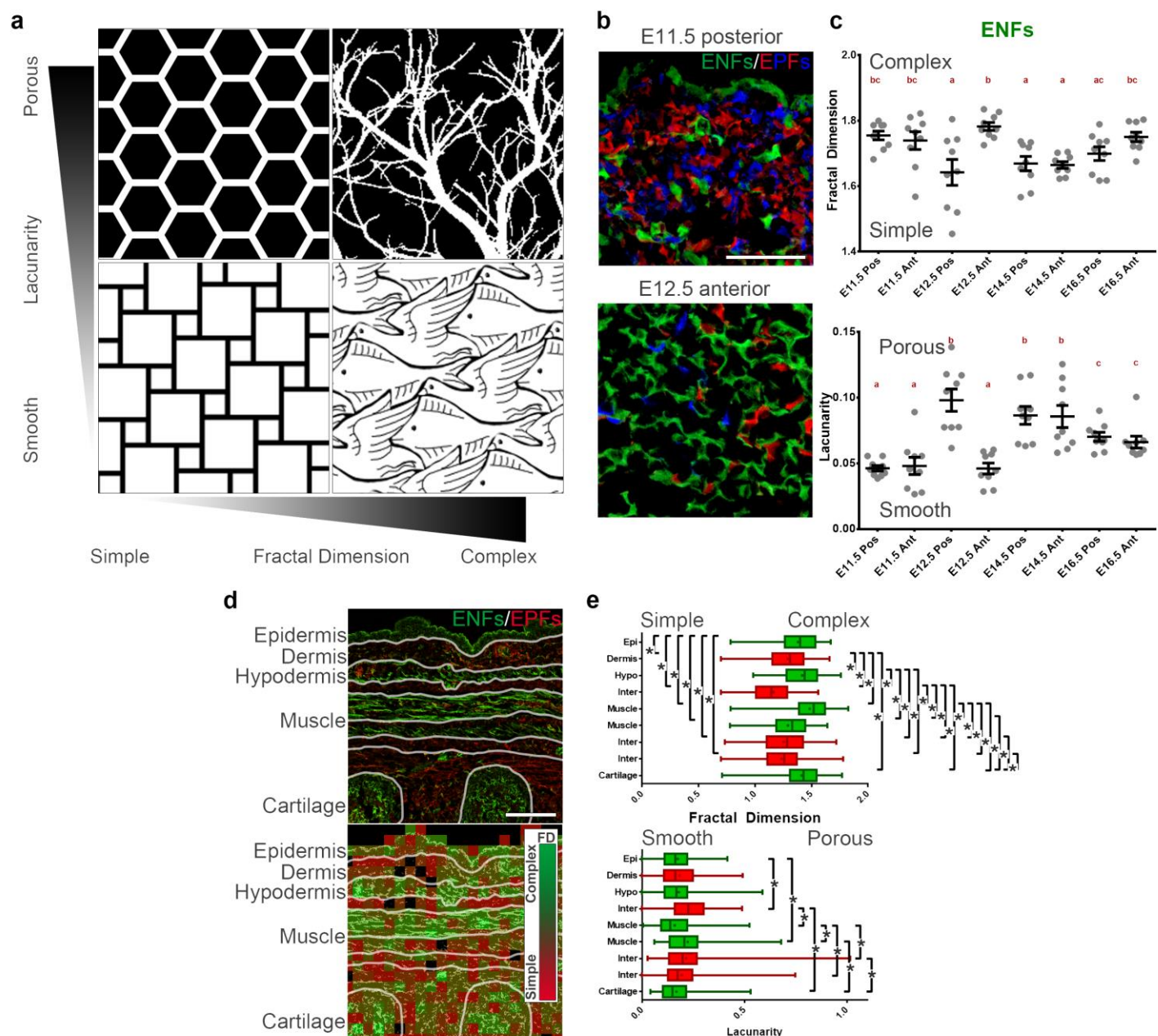


**Supplementary Figure 4**

EPFs actively displace provisional ENF dermis.

3D representations of 24 h time-lapse images of EPF-positive anterior region in E12.5 *En1<sup>Cre</sup>;R26<sup>mTmG</sup>* embryo (up). Max projection of whole live embryo showing the area analyzed (down). Scales: 100  $\mu$ m and 500  $\mu$ m, respectively. Images are taken from the one representative video used for cell tracking analysis showed in Figure 3.

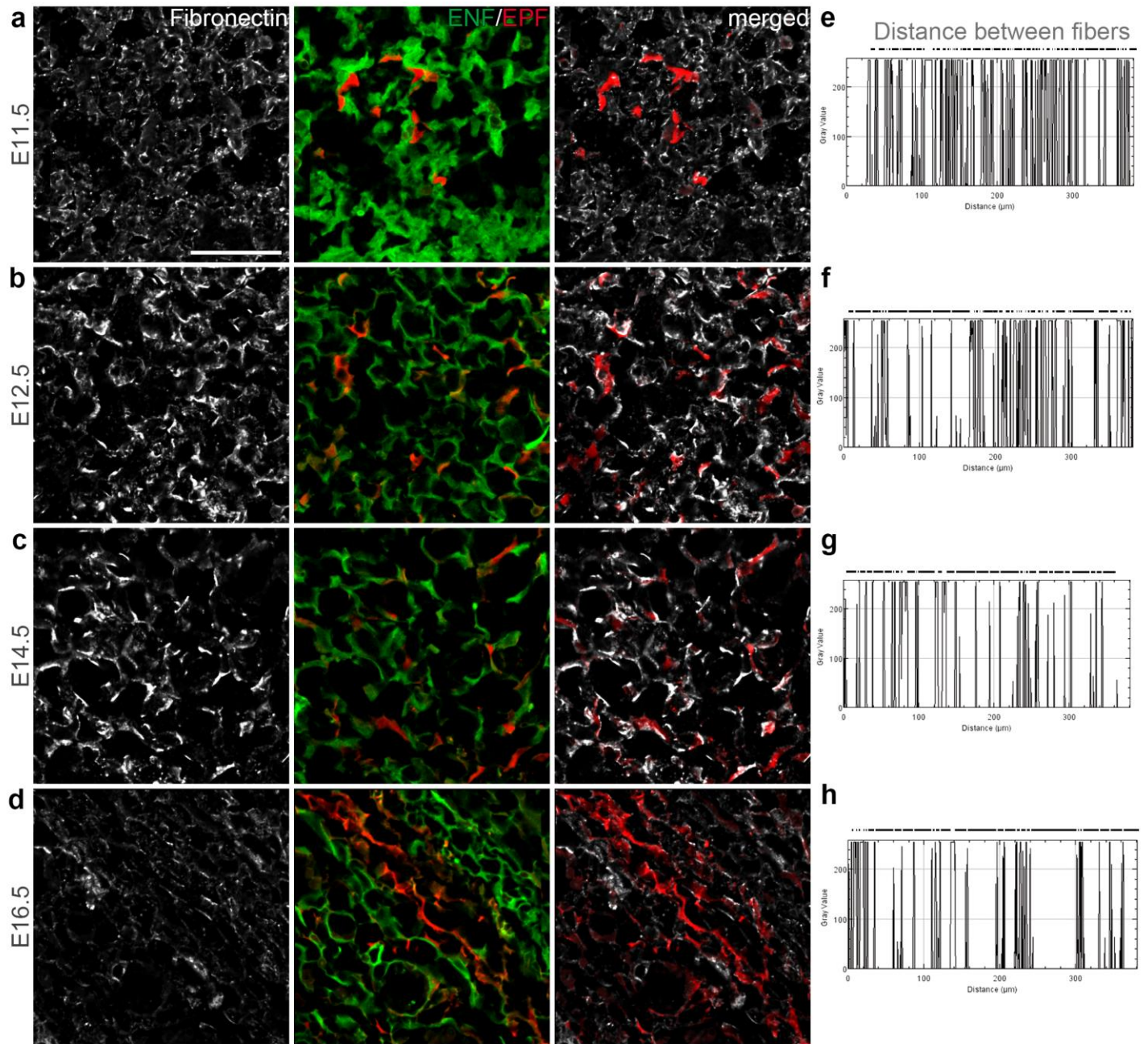




## Supplementary Figure 5

Fractal analysis of ENFs organizations during development. and subsampled fractal analysis.

**a**, Graphical representation of the quantitative assessment of complexity and porosity in 2D images by Fractal analysis. **b**, Representative confocal images of clumped posterior E11.5 EPFs (up), and stretched anterior E12.5 (down) from *En1<sup>Cre</sup>;R26<sup>VT2/GK3</sup>* embryos. **c**, Fractal dimension (up) and lacunarity (down) values derived from ENFs of different regions and developmental stages. Mean  $\pm$  SEM.  $n = 9$  optical fields of anterior or posterior regions at each developmental stage. RM ANOVA,  $p < 0.05$ , Newman-Keuls test. **d**, Subsampled (local) fractal analysis (right) of low-power magnification confocal images of E16.5 *En1<sup>Cre</sup>;R26<sup>VT2/GK3</sup>* embryos (left). Scale: 50  $\mu\text{m}$ . **e**, Fractal dimension (up) and lacunarity (down) values derived from ENFs of different regions and developmental stages,  $n > 60$  subsampled values pooled from three confocal images. ANOVA, Tukey test,  $*p < 0.05$ . Box and whiskers plots with minimum, lower quartile, median, upper quartile, and maximum. The exact  $p$  values are listed in Supplementary Table 1.

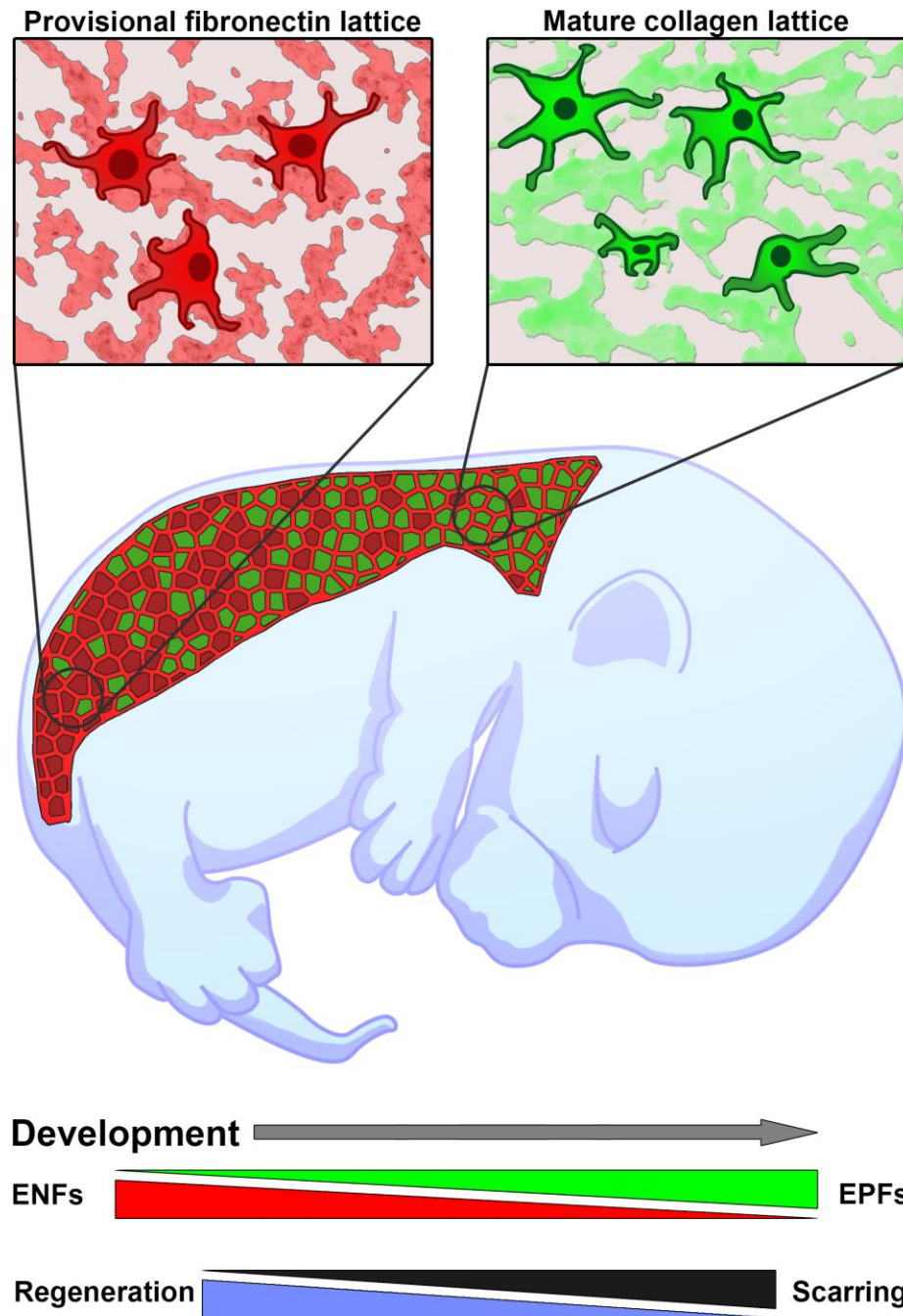


### Supplementary Figure 6

Fibronectin matrix stiffens concurrent with EPF expansion.

a-d, Immunofluorescence for Fibronectin in E11.5 (a), E12.5 (b), E14.5 (c), or E16.5 (d) *En1<sup>Cre</sup>;R26<sup>VT2/GK3</sup>* embryos. e-h, Representative linear profiles of diagonal lines on the Fibronectin signal from E11.5 (e), E12.5 (f), E14.5 (g), or E16.5 (h) images. Dashed lines above the plots represent the calculated distances between fibers. Scale: 50 μm. Images are representatives of 3 optical fields.





**Supplementary Figure 7**

The fibroblastic lineage replacement drives the transition of dermal response to injury from regeneration to scarring.

ENFs are the primary sculptors that drive dermal lattice development and regeneration during early development, and that their cell lineage declines during development. EPFs that produce mature matrix fibres expand concurrently, and predispose back-skin to scarring.



**Supplementary Table 1**

The statistical reports for data showed in Figures 1, 4, 5, and 7 and Supplementary Figures 3 and 5.





### Video 1

EPFs arch in the mouse developing embryo.

3D reconstruction of an *En1*<sup>Cre</sup>; *R26*<sup>VT2/GK3</sup> E12.5 embryo showing the EPFs formations across the dorsum of the embryo. Note that the EPFs at the anterior regions of the embryo showed cells migrating from the dermomyotome. Green: Autofluorescence, Magenta: EPFs.

## Video 2

EPFs actively displace ENFs.

3D reconstruction of time-lapse imaging of an *En1<sup>Cre</sup>;R26<sup>mTmG</sup>* E12.5 embryo at the anterior region of the EPFs arch showing that EPFs migration actively displaces ENFs-provisional dermal cyto-architecture. Green: EPFs, Red: ENFs.



### Video 3

EPFs actively displace ENFs (Only ENFs).

3D reconstruction of time-lapse imaging of an *En1<sup>Cre</sup>;R26<sup>mTmG</sup>* E12.5 embryo at the anterior region of the EPFs arch showing that ENFs-provisional dermal cyto-architecture is displaced. Red: ENFs.